**Rare Metal Materials and Engineering**
Volume 50, Issue 1, January 2021
Available online at www.rmme.ac.cn

Science Press

**Cite this article as:** Rare Metal Materials and Engineering, 2021, 50(1): 0014-0022.

ARTICLE

# Static Recrystallization Behavior of Deformation Induced Inconel 625 Superalloy Pipe

**Chen Jianjun [1,2], Ding Yutian [1,2], Gao Yubi [1,2], Ma Yuanjun [1,2], Wang Xingmao[1,2], Yan Kang[1,2]**

*[1] School of Material Science and Engineering, Lanzhou University of Technology, Lanzhou 730050, China; [2] State Key Laboratory of Advanced Processing and Recycling of Nonferrous Metals, Lanzhou University of Technology, Lanzhou 730050, China*

**Abstract:** The cold deformation and recrystallization behavior of Inconel 625 superalloy were studied by compression deformation at room temperature and recrystallization annealing. The strain distribution, grain size change, microstructure and texture evolution during cold deformation, as well as recrystallization fraction, grain sizes, microstructure and texture evolution of cold deformed Inconel 625 superalloy during recrystallization annealing were analyzed by EBSD technique. Results show that Inconel 625 superalloy has good plasticity when the deformation is 35%~65%. With the increase of deformation, the grain size decreases and the strain distribution is more uniform; {111}<112> texture and {110}<001> texture are gradually weakened, while the {001}<110> texture and the {112}<111> texture are slightly enhanced. After recrystallization annealing treatment of cold deformed Inconel 625 superalloy, the recrystallization fraction increases with the increase of annealing temperature and holding time. With the increase of deformation, the annealing temperature decreases when complete recrystallization with finer grains occurs. When the deformation is 35%, the recrystallization process is mainly transformation from {112}<111> texture and {123}<634> texture into {110}<112> texture, {001}<100> texture and {124}<211> texture. With the increase of deformation amount to 50% and 65%, the {123}<634> texture produced by cold deformation transforms into {124}<211> texture during recrystallization.

**Key words:** Inconel 625 superalloy; EBSD; cold deformation; recrystallization; microstructure; texture evolution

Inconel 625 superalloy is a solution strengthened Ni-Cr based alloy with Mo and Nb as main strengthening elements. It can be used to manufacture extruded pipes, extruded bars, rolled plates, forgings and other materials, and has been used in the fields of aero engines, gas turbine engine and nuclear power equipment, because the superalloy has excellent corrosion resistance, oxidation resistance, good mechanical properties from room temperature to 980 °C, processing properties, and good welding performance[1-9]. It is the manufacturing material of key parts in the fields of aviation, aerospace, nuclear energy, petroleum and chemical industry [10,11]. The Inconel 625 hot-extruded pipe needs to undergo cold deformation and recrystallization annealing to obtain a finished pipe with uniform structure and good mechanical properties [2,12,13]. In the process of cold deformation, with the increase of the amounts of deformation, the deformation resistance caused by work hardening increases, and there are a large number of dislocation-based crystal defects in the deformed microstructure, and a certain storage amount of energy is retained in the deformed alloy. The crystallization annealing process can eliminate the influence of work hardening and obtain an alloy structure with uniform structure, refine grains and thermal stability[14,15]. Since the stacking fault energy of the nickel-based deformed superalloy is low, it is easy to form a stacking fault, and the width of the stacking fault is widened, which makes the cross-slip of dislocations difficult, resulting

Received date: January 10, 2020
Foundation item: National Key Research and Development Program of China (2017YFA0700703); National Natural Science Foundation of China (51661019)
Corresponding author: Ding Yutian, Ph. D., Professor, State Key Laboratory of Advanced Processing and Recycling of Nonferrous Metals, Lanzhou University of Technology, Lanzhou 730050, P. R. China, E-mail: dingyt@lut.edu.cn

in the occurrence of twin deformation, and forming a large number of deformed twins[16,17]. After recrystallization annealing, a large number of annealing twins will be produced in the cold deformed alloy structure. The annealed twin boundary is a coherent grain boundary which is a special large angle grain boundary with low interfacial energy, good thermal stability and mechanical stability properties, and this low interfacial twinning plays an extremely important role in the strength and plasticity of the material [18,19]. Therefore, the use of suitable cold deformation and recrystallization annealing treatment to control the structure of Inconel 625 superalloy is of great significance for obtaining good finished pipe.

At present, many researchers on the dynamic crystallization behavior of nickel-base superalloys have been reported[20-24]. Hot deformation is an important forming method for nickel-based deformed superalloys, and the microstructure and properties of nickel-based superalloys during the thermal processing mainly undergo dynamic recrystallization. The results of the study by Li et al[20] show that the dynamic recrystallization mechanism shifts from discontinuous dynamic recrystallization to continuous with the increase of deformation temperature and the decrease of strain rate when Inconel 625 superalloy undergoes thermal deformation, and the fully dynamic recrystallization structure is equiaxed grains accompanied with twins. The results of the study by Jia et al[23] show that the disappearance and formation of twin boundaries in Inconel 625 superalloy are closely related to the grain growth at different strain rates and deformation temperatures, and the dynamic recrystallization process greatly accelerates the grain boundary migration speed and easily produces new twin boundaries. The current reports on static recrystallization are mainly focused on the annealing process in the late stage of thermal deformation [25,26]; with the completion of dynamic recrystallization, static recrystallization will occur due to the small amount of deformation storage energy and higher temperature, so as to obtain the alloy with stable structure.

Cold deformation and heat treatment are important measures in the subsequent processing of nickel-based deformed superalloys. Our research group has studied the cold deformation and heat treatment of Inconel 625 superalloy, and results show that cold deformation, annealing temperature and annealing time are the main factors affecting the static recrystallization of the alloy. A large number of annealing twins are obtained by annealing treatment, and the ratio of low energy grain boundaries in the alloy structure is improved, which can hinder the connectivity between random grain boundaries, and the invalidation at the grain boundary is hindered or retarded, thereby optimizing the grain boundary of the superalloy, and the optimization of the grain boundary character distribution of Inconel 625 superalloy is mainly achieved by twinning boundaries formed during the recrystallization process [27-30]. However, there are few reports on the static recrystallization behavior of nickel-based superalloys treated by cold deformation and recrystallization annealing. Therefore, based on the previous research, the static recrystallization behavior of Inconel 625 superalloy after cold deformation and annealing, and the evolution of structure and texture during the whole process were further studied by electron backscatter diffraction (EBSD) technique.

## 1 Experiment

The experimental material was Inconel 625 superalloy hot extruded pipe with a size of $\Phi$159 mm×18 mm, whose major chemical composition (wt%) was 60.63Ni-21.77Cr-8.79Mo-3.75Nb-3.68Fe-0.4Ti-0.21Al-0.2Mn-0.19Co-0.12Si-0.042C. After solution treatment at 1150 °C/1 h/AC, the sample was taken along the radial direction of the tube wall, and a cylindrical sample with a size of $\Phi$6 mm×9 mm was cut by wire cutting, and the surface was sanded with sandpaper. WDW-100D electronic universal material testing machine was used for room temperature compression test. The strain rate was 0.1 $s^{-1}$, and the compression deformation was 35%, 50% and 65%. Subsequently, the compressed sample was annealed, the annealing temperatures were 1080, 1100 and 1120 °C, and the holding time was 5, 10 and 15 min, followed by air cooling (AC).

The cold-deformed and annealed specimens were cut along the axis by a wire-cutting machine, and then mechanically ground and polished, followed by electropolishing in a mixed solution of 20% $H_2SO_4$+80% $CH_3OH$. The electrolytic voltage was 20 V and the time was 30 s. Quanta FEG 450 thermal field emission scanning electron microscopy (SEM) equipped with INCA Channel 5 software and EBSD accessories was used to observe EBSD data, and the experimental results were analyzed.

## 2 Results and Discussion

### 2.1 Cold deformation

Fig.1 shows the microstructure of Inconel 625 superalloy pipe after solution treatment at 1150 °C/1 h/AC. It can be seen that the microstructure of the solution-annealed Inconel 625 superalloy is a mixed crystal structure composed of typical equiaxed grains and annealing twins. The grain boundary angle of equiaxed grains is 120°, and the grain size is 31.03 μm. The annealing twins mainly consist of transgranular twins and suspended twins. The two ends of the transgranular annealing twin grow up with the grain boundary migration, which is the coherent grain boundary, and the essence of the formation is stacking fault. However, the suspended annealing twin stops inside the grain, the inner end of the grain is a non-coherent interface, and the formation mechanism is the movement of the partial dislocations according to the polar axis [15]. The interfacial energy of annealing twins is low, the interfacial is relatively stable, and the twin boundary plays a role in dividing grains.

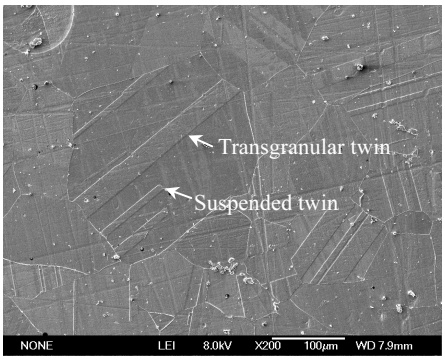


Fig.1 Microstructure of Inconel 625 superalloy after solution treatment

It can be learn from Fig.1 and previous research that Inconel 625 superalloy after solution treatment has relatively large equiaxed grain size and a low yield strength [28,31]. The compression tests at room temperature of Inconel 625 superalloy after solution treatment with different amounts of deformations were carried out, and the microstructure is shown in Fig.2. We can learn from the figure that as the cold compression deformation progresses, the crystal grains are elongated along the direction perpendicular to the compression direction, and the crystal grain shape gradually changes from flat to fibrous with the increase of the deformation amounts. The grain size (including twins) is measured by EBSD using Channel 5 software, and it is reduced from 12.56 μm to 10.03 μm with the increase of the deformation amounts. Our previous research of the grain boundary character distribution during deformation process is shown in Fig.2d [32]. The fraction of high angle grain boundary (the adjacent grain misorientation angle $\theta$>15°) decreases with the increase of cold deformation amounts. However, the fraction of low angle grain boundary (the adjacent grain misorientation angle 2°<$\theta$<15°) and twin boundary increase with the increase of deformation. The results show that with the increase of cold deformation, the degree of work hardening and dislocation density increase, and the deformation changes from slip deformation to twin deformation, because Inconel 625 superalloy has low stacking fault energy. At the beginning of deformation, the grains are deformed coordinately through multi-slip, and with the increase of dislocation, the dislocation density increases, leading to the decomposition of perfect dislocations to form partial dislocations, and the width of stacking fault is widened. In order to realize the cross-slip of extended dislocations, the unit dislocations must be bundled together, so that the slip of dislocations can be suppressed, leading to twinning deformation and forming deformation twins in crystal structure [33,34]. By changing the orientation of the crystal, twinning makes the system which is difficult to slip easier to slip, and the slip takes place inside the twin, so that the plastic deformation can be continued.

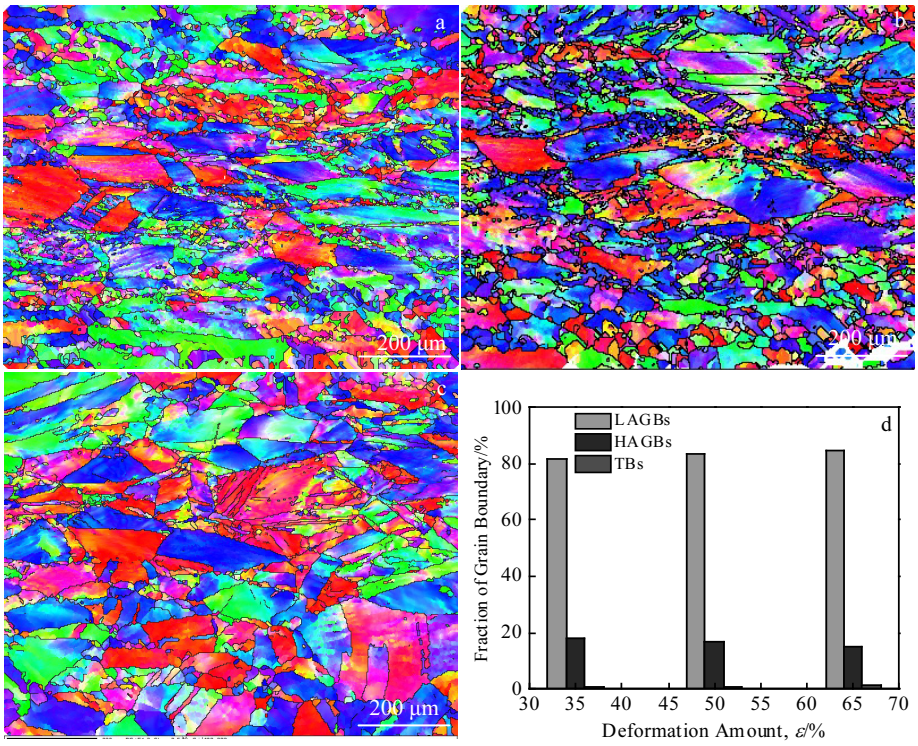


Fig.2 Microstructures (a~c) and grain boundary characteristics (d)[32] of Inconel 625 superalloy with different deformation amounts: (a) 35%, (b) 50%, and (c) 65%

After the cold compression deformation of the Inconel 625 superalloy, a part of the stress remains in the metal due to the non-uniform deformation of the grains or subgrains. Strain contouring of Inconel 625 superalloy under cold deformations of $\varepsilon$=35%, $\varepsilon$=50% and $\varepsilon$=65% is shown in Fig.3, where blue denotes low strain zone and red denotes high strain zone. It can be seen that the low strain region is uniformly distributed in the crystal, nevertheless the high strain regions are mainly distributed near the grain boundary, and as the deformation amount increases, the strain distribution tends to be uniform in the crystal. It is because in the cold deformation process, the grains which are beneficial to the orientation of slip begin to slip first, the dislocations on the slip surface move continuously along the slip surface, and the moving dislocations are blocked at the grain boundary, resulting in the formation of the dislocation pile-up group, and the dislocation pile-up group will cause a great stress concentration, as shown in the high strain region near the grain boundary [34,35]. When the deformation amount is small, some grains have large deformation degree with high dislocation density, while some grains have small deformation degree with low dislocation density, which causes the non-uniform deformation of Inconel 625 superalloy. With the increase of deformation amount, the grains coordinate with each other, and the deformation tends to be uniform, which suggests that the deformation amount increases and the strain distribution changes from non-uniform to uniform. With the increase of deformation, the residual stress increases and exists in crystals in the form of deformation storage energy, which provides a driving force for static recrystallization during subsequent annealing.

## 2.2 Static recrystallization

The main factors affecting static recrystallization are deformation, annealing temperature and holding time. Therefore, the recrystallization behavior of Inconel 625 superalloy under different deformation amounts was studied at different annealing temperatures and holding time. The static recrystallization fractions under different conditions were analyzed by Channel 5 software, and the static recrystallization fraction maps under deformation amounts of 35%, 50%, and 65% are shown in Fig.4. When the static recrystallization fraction is greater than 95%, it is considered that complete static recrystallization occurs. It can be seen from Fig.4 that as the annealing temperature and holding time increase, the recrystallization fraction increases. The larger the deformation degree, the greater the storage energy, and the lower the temperature at which the Inconel 625 superalloy undergoes complete static recrystallization.

When the deformation is 35%, complete static recrystallization occurs at 1120 °C/10 min. When the deformation amount is 50%, complete static recrystallization occurs at 1120 °C/5 min; when the deformation amount is 65%, complete static recrystallization occurs at 1100 °C/15 min and 1120 °C/10 min. Fig.5 shows the microstructure of Inconel 625 superalloy during complete static recrystallization, in which red indicates recrystallized grains, yellow represents subcrystals, and blue represents deformed grains. It can be seen that the structure of

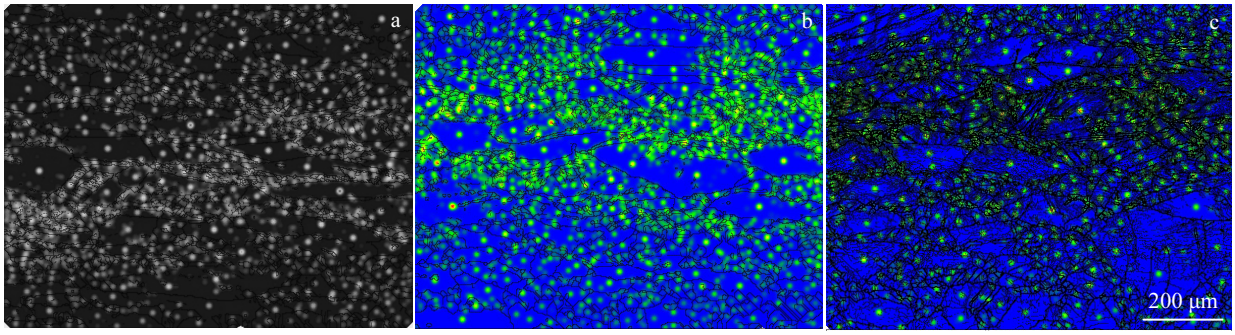


Fig.3 Strain contouring of Inconel 625 superalloy under different deformation amounts: (a) $\varepsilon$=35%, (b) $\varepsilon$=50%, and (c) $\varepsilon$=65% [32]

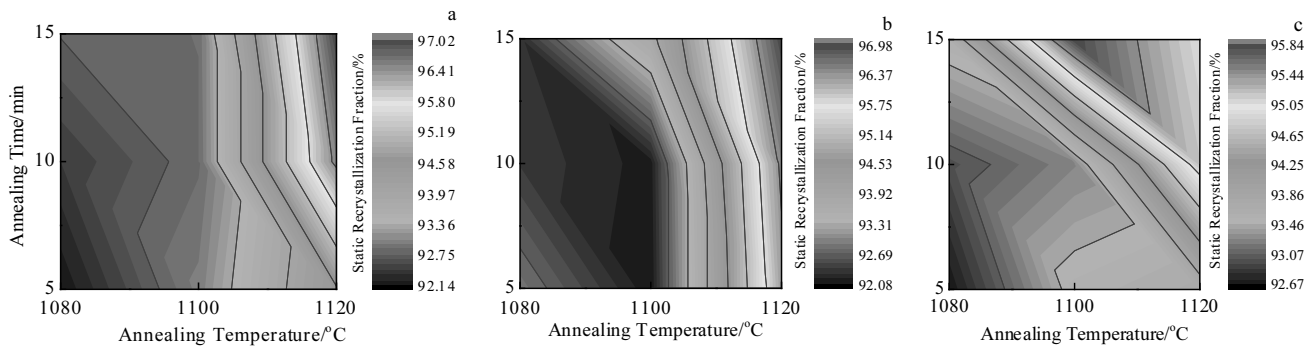


Fig.4 Static recrystallization fraction maps under different deformation amounts: (a) $\varepsilon$=35%, (b) $\varepsilon$=50%, and (c) $\varepsilon$=65%

Inconel 625 superalloy is composed of fine equiaxed grains, a lot of transgranular annealing twins and suspended annealing twins after complete static recrystallization. The grain sizes measured by the Channel 5 software are 17.206, 15.681, 14.516, and 14.1 μm, indicating that the larger the deformation, the smaller the grain size after complete static recrystallization. This is because as the amount of deformation increases, the deformation storage energy increases, the recrystallization nucleation rate increases, and the recrystallized grain size is fine [14]. When the deformation amount is 35%, 50%, and 65%, the partial recrystallization of Inconel 625 superalloy occurs at 1080 °C/5 min, as shown in Fig.6. At this time, recrystallization has been mostly completed, and all the alloy structure consists of a large amount of recrystallized structure (93%), a small amount of subgrain (6.9%) and deformed grains (0.1%). The subcrystal and subcrystal clusters are observed under different deformation amounts, which indicate that the nucleation mechanism of the Inconel 625 superalloy in the late stage of recrystallization is the subcrystal nucleation.

### 2.3 Texture evolution

The orientation distribution function (ODF) section diagram can be used to observe and to quantitatively analyze the texture evolution of materials in different states. Particular emphasis was placed on the ODF sections at $\varphi_2$=45° and $\varphi_2$=65° which can demonstrate the common face-centered cubic (fcc) deformation

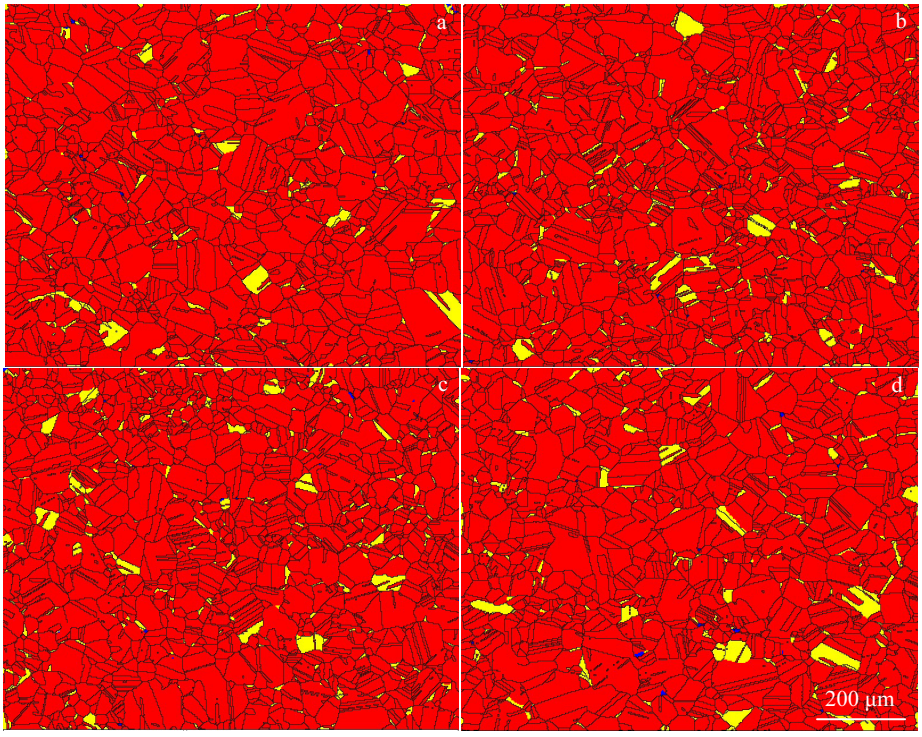


Fig.5 Complete static recrystallization structures of Inconel 625 superalloy under different deformation amounts at different annealing temperatures and holding time: (a) 35%, 1120 °C/10 min; (b) 50%, 1120 °C/5 min; (c) 65%, 1100 °C/15 min; (d) 65%, 1120 °C/10 min

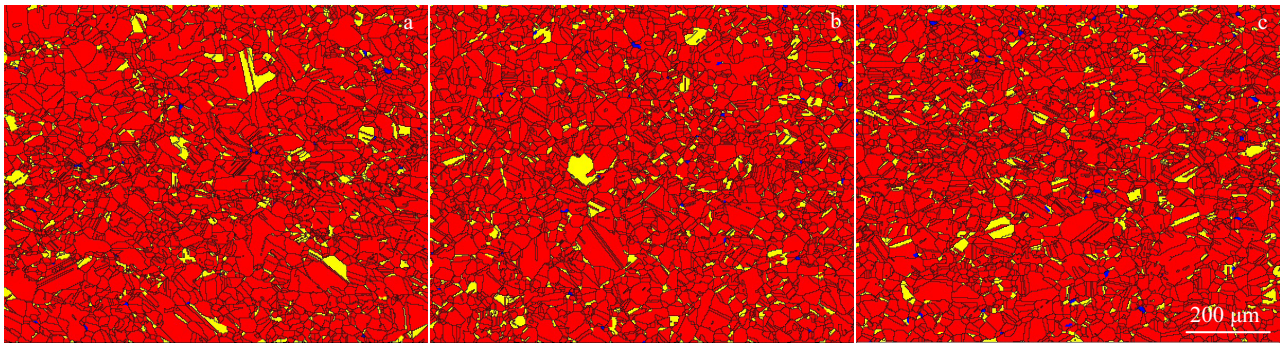


Fig.6 Partially recrystallized structures of Inconel 625 superalloy under different deformation amounts at different annealing temperatures and holding time: (a) 35%, 1080 °C/5 min; (b) 50%, 1080 °C/5 min; (c) 65%, 1080 °C/5 min

texture features. Fig.7a presents the major components and their positions in the selected ODF sections. The ODF sections at $\varphi_2$=45° of Inconel 625 superalloy deformation samples are calculated and depicted by the Channel 5 software in Fig.7b~7d. When the deformation amount of Inconel 625 superalloy is 35%, there are mainly strong {112}<111> texture and {111}<112> texture, weak {001}<110> texture, {110}<001> texture and {123}<634> texture. The orientation {112}<111> and {011}<211> are both stable orientations when the fcc metal is deformed by slip, but the flow of grains towards orientation {011}<211> will result in larger shear strain around normal direction, which makes it difficult for grains to reach orientation {011}<211>, and then the main flow direction is orientation {112}<111>. The {112}<111> texture is the twin element of the fcc metal, when twinning deformation occurs in a grain with orientation {112}<111>, and the orientation of the grain will change from orientation {112}<111> to its twinning position orientation {552}<115>, and then through dislocation slip, the orientation {011}<100> to orientation {011}<211> will flow to orientation {011}<115> [36,37]. Similar to the deformation amount of 35%, when the deformation amount is 50% and 65%, the main existing textures in the alloy are {112}<111>, {111}<112>, {001}<110>, {123}<634> and {110}<001> textures. Combined with the ODF sections diagram shown in Fig.7, it can be seen clearly that with the increase of the deformation, {111}<112> texture and {110}<001> texture are gradually weakened, while the {001}<110> texture and {112}<111> texture are slightly enhanced, indicating that the stable orientation of Inconel 625 superalloy during cold compression is {001}<110> and {112} <111>. This is because the {111}<110> slip system is preferentially activated during the cold compression process of the alloy, and the slip system is actuated to cause the grain orientation to flow toward the orientation {001}<110> and {112}<111>. In the vicinity of the orientation {001}<110> and {112}<111>, the orientation factor of the slip system which causes the grain orientation to rotate in different directions during the deformation process is the same, so that the stable orientation at the time of cold compression is {001}<110> and {112}<111>.

After recrystallization annealing, unstable deformed grains disappear and stable recrystallized grains form. The recrystallization process is the process of nucleation and growth, and recrystallization causes recrystallized texture in the material. Fig.8 shows the ODF sections at $\varphi_2$=45° under different annealing treatments with different deformation amounts. When the deformation amount is 35%, it can be seen from Fig.8a that as the recrystallization process progresses, the {112}<111> texture and the {111}<112> texture are gradually weakened, and {001}<100> texture, {110}<112> texture and {124}<211> texture are gradually enhanced. When the annealing temperature is 1120 °C and holding time is 10 min, the alloy undergoes

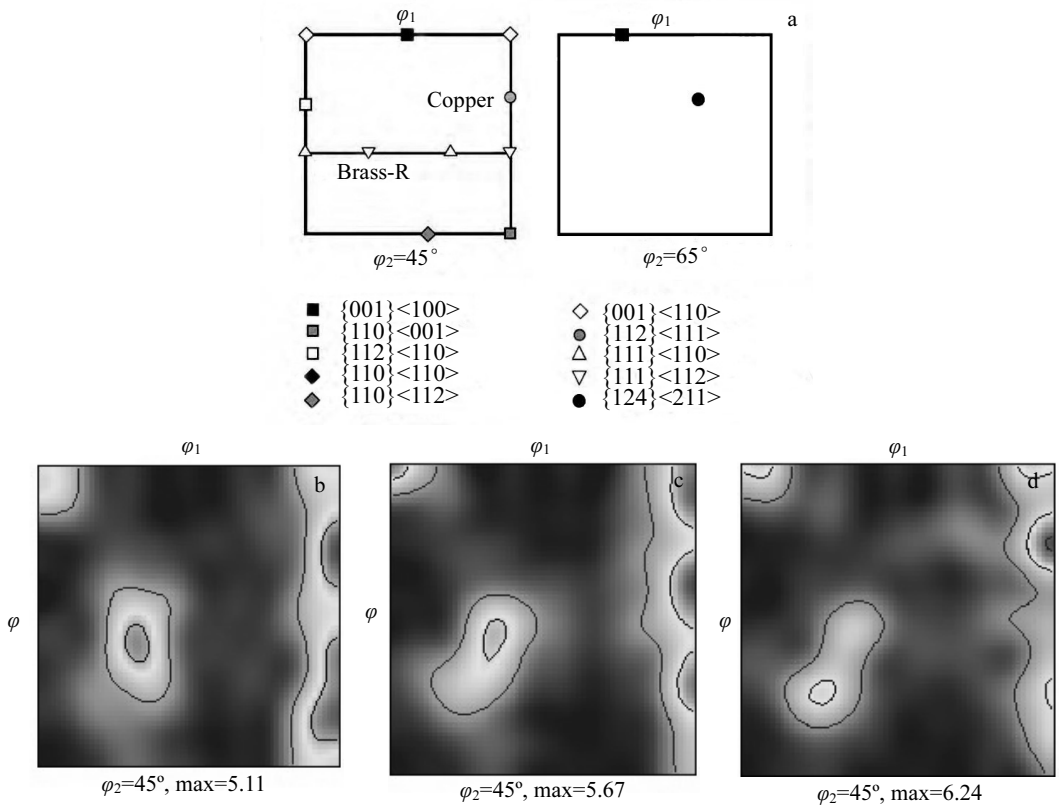


Fig.7 Major texture components and their positions in the ODF sections (a) and ODF sections at $\varphi_2$=45° under different deformation amounts: (b) 35%, (c) 50%, and (d) 65%

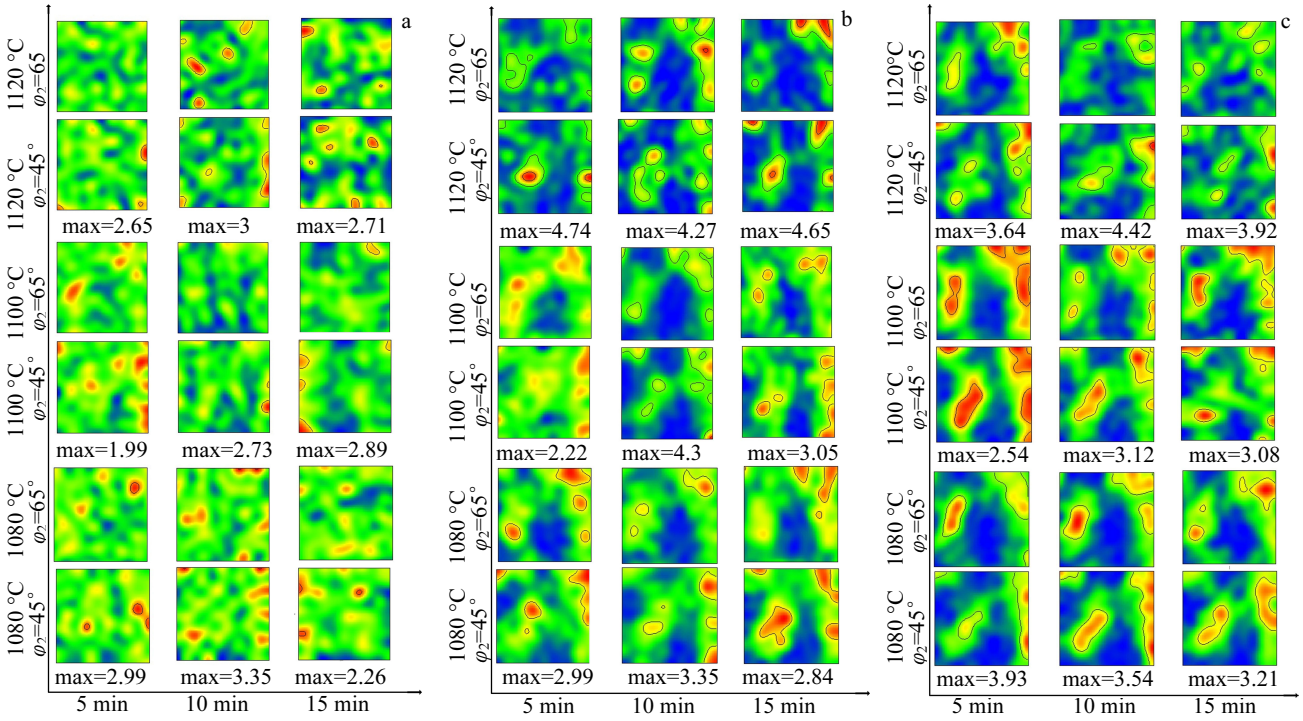


Fig.8 Misorientations measured under different deformation amounts: (a) 35%, (b) 50%, (c) 65%

complete static recrystallization. At this time, there are mainly {001}<110> texture, {112}<111> texture, {111}<112> texture, and weaker {001}<100> texture, {110}<112> texture, {110}<001> texture and {124}<211> texture in the alloy. After holding for 15 min, the recrystallization texture in the alloy is mainly composed of {001}<100> texture, {110}<112> texture, a few of {112}<111> texture and {110}<001> texture. It can be seen that the recrystallization annealing process of Inconel 625 superalloy under small deformation with different annealing systems results in the process of complete static recrystallization from aggregation to dispersion and then aggregation. The recrystallization process is mainly transformed from {112}<111> texture and {123}<634> texture into {110}<112> texture, {001}<100> texture and {124 }<211> texture. Studies have shown that [38] in the fcc metal, when there is a 40° <111> relationship between the deformed matrix and the growing recrystallized grains, the growth rate reaches a maximum value. Fortunately, both the {001}<100> texture and {124}<211> textures have 40° <111> relationship with {123}<634> texture. When holding for 15 min, it is found that {111}<112> texture is weakened and {110}<112>texture is enhanced. It is obvious that {111}<112> texture provides a large number of nucleation sites for grains with orientation{110}<112>. When the deformation is 50% and 65%, the recrystallization texture is more concentrated, as shown in Fig.8. When the deformation amount is 50%, and annealing temperature and holding time is 1120 °C/5 min, it can be seen from the ODF sections that when complete recrystallization occurs, the texture in the alloy mainly accumulates near the {111}<112> texture, while a small amount of {001}<110> texture, {110}<001> texture, {112}<111> and {124}<211> texture exist, and the recrystallization texture changes little with the prolongation of holding time. At the same time, when the deformation amount is 65%, texture evolution during different annealing systems has a similar phenomenon when the deformation amount is 50%. Obviously, with the increase of deformation, the {123}<634> texture generated by cold deformation is restrained to {001}<100> texture during recrystallization, which is transformed into {124}<211> texture. In the meantime, with the change of holding time and annealing time, the formation of {110}<112> texture is suppressed at higher deformation amount. According to the analysis[39], with the increase of deformation, due to the coordinated deformation of grains and the large storage energy in deformed metals with uniform strain distribution, the {123}<634> texture is more likely to transform into {124}<211> texture.

## 3 Conclusions

1) During the deformation process of Inconel 625 superalloy with a compressive deformation amount of 35%~65% at room temperature, the dominant is slip deformation, and only a small amount of twin deformation occurs. With the increase of deformation, the grain size decreases, the grains coordinate with each other, the structure uniformly deforms into fibrous structure, the strain distribution tends to be uniform, and the high strain zone is mainly concentrated near the grain boundary.

2) The factors affecting the recrystallization of Inconel 625 su-

peralloy mainly include deformation amount, annealing temperature and holding time. With the increase of annealing temperature and holding time, the recrystallization fraction increases. When the deformation amount is 35%, the annealing temperature and holding time gradually increase from 1080 °C/5 min to 1120 °C/15 min, and the recrystallization fraction increases from 92.14% to 97.02%. As the deformation increases, the storage energy increases, which makes the annealing temperature decrease when complete recrystallization occurs as well as smaller recrystallization grain size. When the deformation is 65%, complete static recrystallization occurs at 1100 °C/15 min, the recrystallization grain size is the smallest with an average grain size of 14.1 μm.

3) With the increase of the deformation, {111}<112> texture and {110}<001> texture are gradually weakened, while the {001}<110> texture and {112}<111> texture are slightly enhanced, and the stable orientation of the alloy is {001}<110> and {112}<111>.

4) Static recrystallization occurs after annealing of cold deformed Inconel 625 superalloy. When the deformation amount is 35%, texture evolution during recrystallization process is mainly transformation from {112}<111> texture and {123}<634> texture into {110}<112> texture, {001}<100> texture and {124}<211> texture. As the deformation amount increases to 50% and 65%, the {123}<634> texture produced by cold deformation is transformed into {124}<211> texture during recrystallization, and the formation of {001}<100> texture and {110}<112> texture is inhibited at larger deformation.

## References


1 Ma D, Stoica A D, Wang Z Q *et al. Materials Science & Engineering A*[J], 2017, 684: 47

2 Gao Y B, Ding Y T, Chen J J *et al. Materials Science & Engineering A*[J], 2019, 767: 138 631

3 Comot P, Bocher P, Belanger P. *NDT & E International*[J], 2017, 91: 71

4 Wang L Y, Li H P, Liu Q Y *et al. Journal of Alloys and Compounds*[J], 2017, 703: 523

5 Ding Y T, Meng B, Gao Y B *et al. Rare Metal Materials and Engineering*[J], 2019, 48(5): 1605 (in Chinese)

6 Ding Y T, Gao Y B, Dou Z Y *et al. Acta Metallurgica Sinica*[J], 2017, 53(6): 695 (in Chinese)

7 Ma Y J, Ding Y T, Liu J J *et al. Rare Metals*[J], 2020, 40(3): 256 (in Chinese)

8 Ma Y J, Ding Y T, Liu J J *et al. Physics and Engineering of Metallic Materials, CMC 2018* [C]. Xiamen: Springer, 2018: 153

9 Ding Y T, Chen J J, Li H F *et al. Materials Reports*[J], 2019, 33(16): 2753 (in Chinese)

10 Guo J T. *Materials Science and Engineering for Superalloys*[M]. Beijing: Science Press, 2008 (in Chinese)

11 China Aeronautical Materials Handbook Compile Committee. *China Aeronautical Materials Handbook*[M]. Beijing: Standards Press of China, 2002 (in Chinese)

12 Wang Z T, Zhang S H, Cheng M *et al. Forging & Stamping Technology*[J], 2010, 35(4): 48 (in Chinese)

13 Jiang H, Dong J X, Zhang M C *et al. The Chinese Journal of Nonferrous Metals*[J], 2017, 27(7): 1385 (in Chinese)

14 Bair J L, Hatch S L, Field D P. *Scripta Materialia*[J], 2014, 81: 52

15 Gao Y B, Ding Y T, Chen J J *et al. The Chinese Journal of Nonferrous Metals*[J], 2019, 29(1): 44 (in Chinese)

16 Yuan Y, Gu Y F, Cui C Y *et al. Journal of Materials Research*[J], 2011, 26(22): 2833

17 Shang S L, Wang Y, Du Y *et al. Computational Materials Science*[J], 2014, 91: 50

18 Jin Y, Lin B, Bernacki M *et al. Materials Science & Engineering A*[J], 2014, 597: 295

19 Yang C L, Zhang Z J, Zhang P *et al. Materials Science & Engineering A*[J], 2018, 736: 100

20 Li D F, Guo Q M, Guo S L *et al. Materials & Design*[J], 2011, 32(2): 696

21 Chen X M, Lin Y C, Wen D X *et al. Materials & Design*[J], 2014, 57: 568

22 Jia D, Sun W R, Xu D S *et al. Journal of Alloys and Compounds*[J], 2019, 724: 196

23 Jia Z, Gao Z X, Ji J J *et al. Advanced Engineering Materials*[J], 2019, 21: 1 900 426

24 Jia Z, Gao Z X, Ji J J *et al. Materials*[J], 2019, 12: 510

25 Chen X M, Lin Y C, Wu F. *Journal of Alloys and Compounds*[J], 2017, 724: 198

26 Lin Y C, Liu Y X, Chen M S *et al. Materials & Design*[J], 2016, 99: 107

27 Ding Y T, Gao Y B, Dou Z Y *et al. Materials Reports*[J], 2017, 31(10): 70 (in Chinese)

28 Ding Y T, Gao Y B, Dou Z Y *et al. Transactions of Materials and Heat Treatment*[J], 2017, 38(2): 178 (in Chinese)

29 Gao Y B, Ding Y T, Chen J J *et al. Chinese Journal of Rare Metals*[J], 2020, 44(7): 673 (in Chinese)

30 Gao Y B, Ding Y T, Chen J J *et al. Rare Metal Materials and Engineering*[J], 2019, 48(11): 3585 (in Chinese)

31 Ding Y T, Ma Y J, Dou Z Y *et al. Materials Reports*[J], 2018, 32(8): 1311 (in Chinese)

32 Gao Y B, Ding Y T, Chen J J *et al. Acta Metallurgica Sinica*[J], 2019, 55(4): 547 (in Chinese)

33 El-Danaf E, Kalidindi S R, Doherty R D. *Metallurgical and Materials Transactions A*[J], 1999, 30(5): 1223

34 Yuan Y, Gu Y F, Cui C Y *et al*. *Advanced Engineering Materials*[J], 2011, 13(4): 296

35 Fan J H, Chen K X, Liang J P *et al. Chinese Journal of Materials Research*[J], 2015, 29(6): 439 (in Chinese)

36 Heye W, Wasserman G. *Scripta Metallurgica*[J], 1968, 2(4): 205

37 Leffers T, Ray R K. *Progress in Materials Science*[J], 2009, 54(3): 351

38 Hu W Y, Chen J C, Liu Er W *et al. Heat Treatment of Metals*[J], 2014, 39(1): 89 (in Chinese)

39 Esmaeilzadeh M, Qods F, Arabi H *et al. International Journal of Fatigue*[J], 2017, 105: 191

# 形变诱导 Inconel 625 合金管材的静态再结晶行为

陈建军[1,2]，丁雨田[1,2]，高钰璧[1,2]，马元俊[1,2]，王兴茂[1,2]，闫　康[1,2]

(1. 兰州理工大学 材料科学与工程学院，甘肃 兰州 730050)

(2. 兰州理工大学 省部共建有色金属先进加工与再利用国家重点实验室，甘肃 兰州 730050)

**摘　要**：通过室温压缩变形与再结晶退火处理研究了 Inconel 625 高温合金冷变形及再结晶行为，采用 EBSD 技术分析冷变形过程中的应变分布、晶粒尺寸变化、组织与织构演变，以及冷变形 Inconel 625 合金再结晶过程中再结晶分数、晶粒尺寸、组织及织构演变。结果表明，Inconel 625 合金在变形量为 35%~65%时具有良好的塑性，随着变形量的增加，晶粒尺寸减小，应变分布越均匀，{111}<112>织构和{110}<001>织构逐渐减弱，而{001}<110>织构和{112}<111>织构略为增强。冷变形 Inconel 625 合金经再结晶退火处理后，随着退火温度升高与保温时间的延长，再结晶分数增大；随着变形量的增大，Inconel 625 合金发生完全再结晶时的温度降低，且发生完全再结晶时的晶粒尺寸变小，变形量为 35%时，再结晶过程主要是{112}<111>织构和{123}<634>织构转变为{110}<112>织构、{001}<100>织构与{124}<211>织构。随着变形量增加到 50%及 65%时，冷变形产生的{123}<634>织构在再结晶过程中转变成了{124}<211>织构。

**关键词**：Inconel 625高温合金；EBSD；冷变形；再结晶；微观组织；织构演变

---

作者简介：陈建军，男，1993 年生，博士生，兰州理工大学省部共建有色金属先进加工与再利用国家重点实验室，甘肃 兰州 730050，E-mail: lutchenjianjun@163.com